# An Innovative Extraction Methodology of Active Deformation Areas Based on Sentinel-1 SAR Dataset: the Catalonia case study

**Zhiwei Qiu[1],*, Oriol Monserrat[2], Michele Crosetto[2], Vrinda Krishnakumar[2], Li Zhou[1]**

[1]Jiangsu Ocean University, Cangwu Road 59, Haizhou District, Lianyungang, China, 222005

[2] Centre Tecnològic de Telecomunicacions de Catalunya (CTTC/CERCA), Geomatics Division, 08860 Castelldefels, Spain; omonserrat@cttc.cat (O.M.); mcrosetto@cttc.cat (M.C.)

*Author to whom correspondence should be addressed; E-Mail: qiuzhiwei-2008@163.com;

**Abstract:** Persistent Scatterer interferometry (PSI) has been proved to be an advanced interferometric SAR (InSAR) technique used to measure and monitor terrain deformation**.** Two of the critical problems with InSAR have been the effect of the refractive atmosphere and decorrelation on the interferometric phases due to long spatial-temporal baseline. The low density of Persistent Scatterers (PS) in non-urban areas affected by spatial-temporal decoherence more seriously has inspired the development of alternative approaches. Sentinel-1 (S1) has improved the data acquisition throughout, and compared to previous sensors, increased considerably the differential interferometric SAR (DInSAR) and PSI deformation monitoring potential. This paper describes an innovative methodology to process S1 SAR data. Different with PSI, its most original part includes two key processing stages: high and low frequency splitting from wrapped phases, prior to atmospheric filtering, and final direct integration to generate the complete deformation with time series (TS) containing linear and nonlinear components. The proposed method has two fundamental advantages compared with traditional PSI approach: the final monitoring results with excellent coverage of coherent points and the generation of active maps even for the areas with

serious deformation in short term to break through the inherent limitation of PSI. The effectiveness of the proposed tools is illustrated using a case study located in Catalonia (Spain). This methodology has supposed a definitive step towards the implementation of DInSAR based techniques to support decision makers against geohazards. In this work, the deformation procedures happened in three different areas of the Catalonia (Spain) are presented and analyzed. The maximum accumulated subsidence of over -60cm induced by mining activity can be detected by proposed methodology with nice coverage from January 2017 to January 2019. These reported cases illustrate how DInSAR based techniques can provide detailed terrain deformation for geohazard activity with complex topographical conditions. The active deformation areas (ADA) map can be generated in fast aimed at geohazard risk early warning and management.

**Keywords:** Persistent Scatterer Interferometry; frequency splitting; direct integration; terrain deformation; risk management

## 1. Introduction

This paper is focused on TS deformation extraction by using S1 data with great spatial coverage and high resolution. In the last 30 years, the spaceborne DInSAR technique has received great improvements since it was proposed with L-band Seasat SAR data at first in 1989 (Gabriel et al. 1989). The advanced approach needs large sets of SAR Images is the so-called PSI technique published by Ferretti and co-authors (Ferretti et al. 2001). During last two decades, a wide number of data processing and analysis tools and methods are generated in this period. An excellent review of Spaceborne DInSAR techniques can be found in (Crosetto et al. 2016) which include the classical standard DInSAR, PSI analysis over small areas, full PSI with linear deformation model and with free deformation model, while a specific application of DInSAR for geohazard mapping is presented in (Barra et al. 2017).

Generally, PSI is a powerful radar based remote sensing technique able to monitor displacements of the Earth’s surface (Núria et al. 2018). Among the pioneering techniques, PSI can improve InSAR accuracy by exploiting the persistent scatterers with high spatial-temporal stabilities, nevertheless, this significantly reduces the possibility of InSAR applications in rural areas. The low PS density in non-urban areas has blocked the invention of complementary techniques to PSI. To exploit partially decorrelating areas in TS analysis, all SAR images has been utilized for the interferograms generation even if the baseline between these two acquisitions is longer than the critical length. In this way, poor-quality interferograms with long spatial-temporal baseline can be selected for PSI measurement and high-quality interferograms with short temporal baseline may be discarded to guarantee the independence of atmospheric phase over time. However, the classic PSI approach utilizes the linear deformation model to extract the displacement phases. As a consequence, in the areas where displacements are characterized by non-linear motion, there will be no PSs (K.Pawluszek-Filipiak, 2020) .

Although this advanced technique has experienced a continuous growth, it is important to underline the DInSAR techniques are not universal. The two intrinsic limitations of DInSAR techniques are less density of PS due to coherence loss for long-term deformation monitoring (especially for non-urban area) and phase ambiguities estimation from the wrapped phase. Due to the PS should be considered as stable with respect to a reference point, such as rocky outcrops or hand-made artifacts, the number of them is very limited in mountain areas where always have geohazard phenomenon (e.g., landslide, earthquake). Moreover, the wrapped phases are difficult to estimate ambiguities exactly because the interferograms generated form SAR image pairs include atmosphere, topography, deformation phases and so on (Crosetto et al. 2010) and the phase unwrapping procedure is time costing due to the atmosphere turbulences not suitable to recognize the geohazard quickly.

Having considered the limitation of PSI approach, a procedure for ADA extraction over wide coverage containing coherent points with high density and temporal sampling (the minimum revisiting cycle is six days) for the geohazard management is designed elaborately and carried out in this study. A dataset of C-band S1 images over the Catalonia (Spain) were employed for monitoring measurement, it is worth mentioning the procedures of TS deformation were investigated well by the proposed method based on S1 acquisitions with short spatial-temporal baselines in our work.

The paper is organized as follows. Section 2 describes the proposed workflow and the tools for the TS deformation extraction. The study area input dataset and the main results of the application of the methodology to the test areas are shown in Section 3 and discussed in Section 4. Finally, Section 5 presents the main conclusions.

## 2. Methodology

In this section, the processing chain to derive the TS deformation estimation and ADA maps extraction is illustrated in detail. The proposed procedure can be applied to the data acquired by any satellite SAR sensor. However, it provides the best performances with the S1 characteristic due to its high spatial coverage and temporal resolution.

According to InSAR principle and frequency spectrum analysis (P. Olea et al.2020; Qiu Z et al. 2020), the interferometric phases can be divided into two parts: High Frequency (HF) and Low Frequency (LF). Since the systematic errors caused by the DEM or orbit errors could be corrected by calibration， these errors can be ignored in this study. Hence, the detailed model can be described as follow:

$$\begin{aligned}\varphi &= \varphi_{def} + \varphi_{atmo} + \varphi_{noi} = \Phi_{high} + \Phi_{low} \\ &= (\varphi_{def\_main} + \varphi_{noi})_{high} + (\varphi_{def\_res} + \varphi_{atmo})_{low}\end{aligned} \tag{1}$$

Where $\varphi_{def}$ is the deformation phase, $\varphi_{atm}$ is atmospheric phase and $\varphi_{noi}$ is noise phase, $\varphi_{def\_main}$ is the main part of the deformation phase, and $\varphi_{def\_res}$ represents the residual deformation phase. The noise and atmospheric signals in the interferogram are located at high and low frequency respectively, while the deformation signal exists in the entire frequency spectrum, the deformation phase can be extracted by effective frequency division processing (Daniel R et al., 2013; Bru G et al., 2017). In particular, for this research, the interferograms have been generated using an approach of Persistent Scatter Interferometry chain of the Geomatics (PSIG) Division of CTTC described in (Devanthéry et al. 2014). The general scheme of the procedure, shown as a flowchart in Figure 1, can be divided in several main blocks.

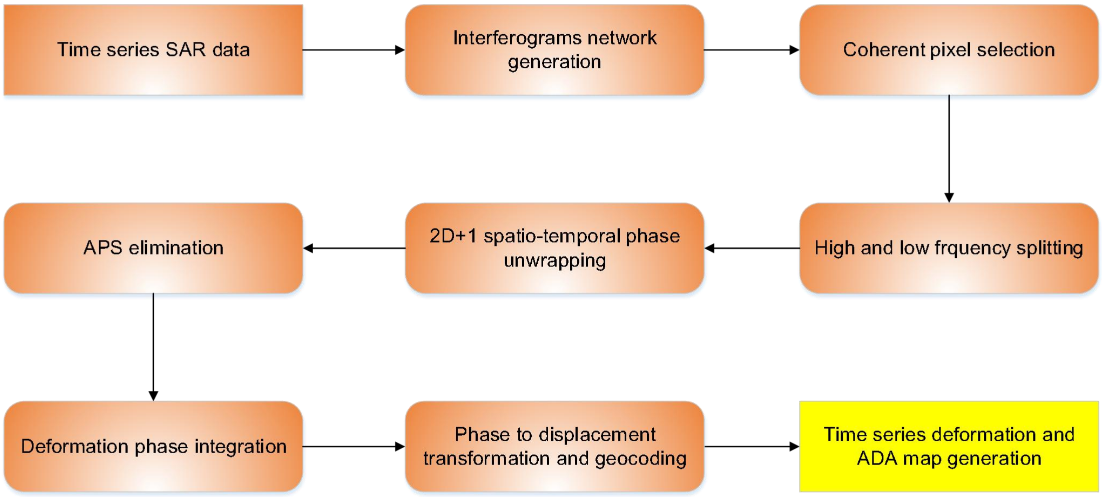


Figure 1. Flow chart of the proposed procedure

### 2.1 *Interferograms network Generation*

To generate interferograms network with short spatial-temporal baseline, several steps should have been done before. This analysis provides key inputs for the network like the minimum temporal baseline to be used since the deformation detection quality could be guaranteed with high coherence. Therefore, the data with same temporal baseline (such as 6 or 12 days) are collected for the interferograms network generation. After extraction from bursts and swaths of S1 dataset, the key step is the image co-registration, which could be very accurate for interferometric phase by means of auxiliary Digital Elevation Model (DEM) before the interferograms generation. After the step of co-registration, the interferograms between the pairs can be created for next steps.

### 2.2 *High and Low frequency splitting and direct integration*

(1) High and Low frequency splitting: Since an interferogram consists of much complex phase information such as deformation, atmosphere and noise. etc., it is very difficult to extract the deformation information form wrapped phases directly and correctly. An innovative approach has been proposed here is to split the consecutive interferograms into two parts: high and low frequency. The noise and displacement phase are treated as HF segment mainly which is useful to accomplish our detection test, and atmospheric phase as LF segment is worthless for our goal, but the residual deformed phases still exist in LF. A proper and empirical threshold is adopted in this step to extract the deformation from the interferograms mainly. However, different thresholds should be evaluated in order to acquire the best separation effect. For example, in the Catalonia test site, only the pixels

with cut off threshold higher than 40 have been selected as HF segment by Butterworth band-pass filtering.

$$\left|H_a(j\Omega)\right| = \frac{1}{\sqrt{1+(\frac{\Omega}{\Omega_c})^{2N}}} \qquad (2)$$

In the above formula, $\Omega$ denotes the frequency, $\Omega_c$ is the cut-off frequency, $N$ is the order. The LF band phase $\Phi_{low}$ dominated by atmospheric phase is separated from the interferogram, and then the HF band phase dominated by deformation phase is separated from the interferogram by conjugation operation, that is $\Phi_{high}=\Phi-\Phi_{low}$ ; the TS interferometric phase sequences corresponding to HF and LF are $\Phi_{high}^{(k)}$ and $\Phi_{low}^{(k)}$ $\forall k \in (1,2,\ldots,N-1)$ respectively, as shown in Figure 2. After HF and LF separation, the Goldstein filter is utilized to adaptively denoise the interferogram to remove the residual noise phase $\varphi_{noi}$ in the HF phase.

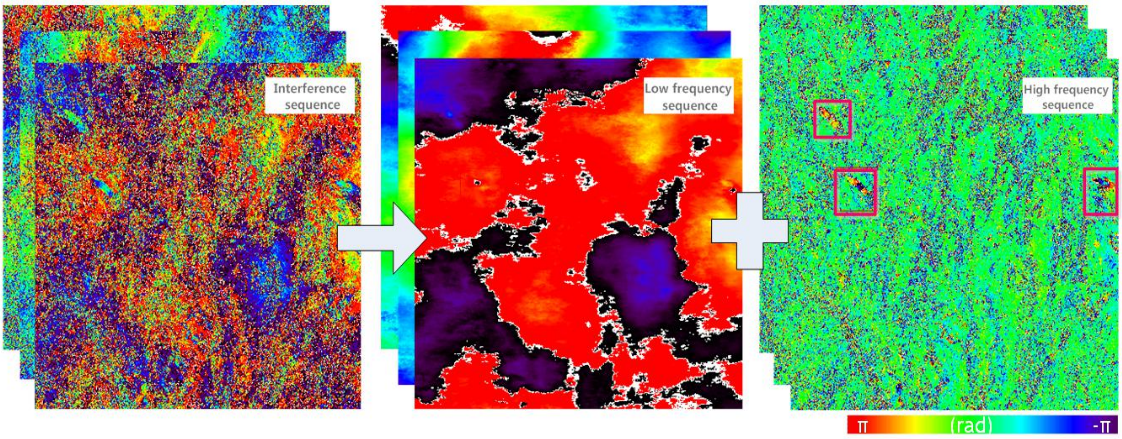


Figure 2. Schematic diagram of high and low frequency band separation

(2) 2D phase unwrapping: Actually, this is a two-step spatial-temporal phase unwrapping approach (Crosetto, M et al, 2007). The phase unwrapping is performed twice in the procedure we proposed here: (i) prior to atmospheric filtering and (ii) during TS deformation generation. In the following, we treat separately these two stages which is a data quality control step. The first stage, which is prior to the atmospheric filtering, can generate the quality index for each pixel in the images. After HF and LF splitting, we start

with a spatial phase unwrapping (2D) performed over the selected set of points and for high and low interferograms separately. For each pixel, the main output is the evolution of the phases with respect to a reference image for each interferogram. The second stage, which is used to generate the TS deformation, can generate the quality index for each image of a given TS deformation. The quality indices are defined by the ratio (Cor_%) between the number of residuals and the total number of interferogram or image for data quality control, if this ratio is above 40%, all the pixels or images are labelled as "not Good" should be discarded form dataset in the subsequent processing steps. Therefore, the 2+1D phase unwrapping can be employed as an analysis tool to guarantee the quality of pixels and interferograms for the TS deformation. In particular, it refers to the so-called 2+1D phase unwrapping described in (Devanthéry et al. 2014).

(3) Direct integration for high and low frequency segment: This procedure can be used to correct the unwrapping errors. A pixel wise processing is performed in this step, which analyses over unwrapped interferometric phases with time series. By an iterative process, exploiting the Single Value Decomposition (SVD) least squares method and adopting an outlier rejection strategy, the matrix used for SVD is built by so-called residuals $R = \Delta\varphi - (\varphi_M - \varphi_S)$ associated with observations of unwrapped interferometric phases. This procedure determines the phases values associated with each SAR image, starting from a stack of interferograms. The high and low frequency combined phase over time is estimated accumulatively for each point as follows:

$$\begin{cases} \varphi_i = \varphi_{i-1} + \Delta\varphi_{i(i-1)} & i = 1 \div N \\ \varphi_0 = 0 \end{cases} \tag{3}$$

Where $\varphi_i$ the accumulated phase at the acquisition is time i, and $\Delta\varphi_{i(i-1)}$ is the interferometric phase between the images i and i-1.

*2.3 Active Deformation Areas (ADA) Extraction*

The main goal of this block is to discover TS deformation of the active areas from interferograms fast and correctly, which is very meaningful for Geo-hazard detection and early warning. In this section, the procedure to detect the active deformation area from interferograms directly without any complex and time-consuming analysis is described. The automatic ADA detection strategy proposed in this article is a robust procedure performed using a set of spatial-temporal filters. In other words, the threshold parameter used just for the S1 should be changed to suit for other SAR sensors. The full procedure consists in the following steps (Figure 3):

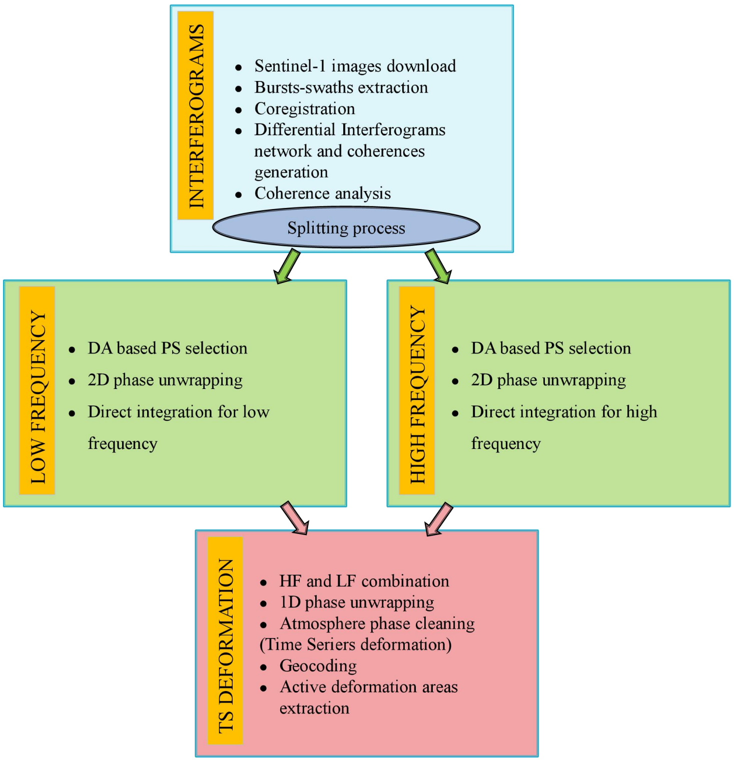


Figure 3. Flow chart of ADA extraction

(1) HF&LF combination: From previous analysis of HF and LF splitting, the most parts of deformation phase are persisted in the HF segment. However, the rest still is contained in the LF segment. Then, these two parts of deformation should be combined for each PS pixel.

(2) 1D phase unwrapping: This is the second step for 2+1D phase unwrapping to check the phase unwrapping consistency done by point wise, exploiting the temporal component of SAR images stack. It is based on an iterative least square (LS) method and the analysis of the LS residuals at each iteration in order to correct the "phase jump".

(3) Atmospheric phase estimation and reduction: The APS is estimated using spatial-temporal filters. The main input is the temporal evolution of the phases (TEP) estimated in the previous step. The estimated APS is removed from the TEP. The remaining phases are then transformed into deformations, obtaining the final TS deformation.

(4) ADA extraction: This is the last of the ADA extraction block after geocoding. It consists of nonlinear TS deformation without any temporal filtering, i.e., regression line estimation. The used method is a valid tool for the character analysis of the deformation phenomena such as

landslide, settlements and so on.

The final output of these blocks above is an ADA maps including, for each point, the accumulated TS deformation along the satellite LOS direction at each acquisition time. The active deformation area could be recognized from the geocoded outputs finally.

## 3 Catalonia Study Results

In this section, several results obtained from the new strategy proposed in this article are presented and discussed. The explained procedure has been applied to the Catalonia area in Spain, and there are different types of geo-disasters such as urban settlement, mining subsidence and mountains landslide or rockslide happened in this study area.

### *3.1 Study Area*

These results were derived from S1 SAR images over Catalonia which is an autonomous community of Spain consisting of four provinces: Barcelona, Girona, Lleida, and Tarragona.

Catalonia has a marked geographical diversity, considering the relatively small size of its territory (Figure 4). The geography is conditioned by the Mediterranean coast, with 580 kilometers (360 miles) of coastline, and large relief units of the Pyrenees to the north. The Catalan territory can be divided into three main geomorphologic units:

(1) The Pyrenees: mountainous formation that connects the Iberian Peninsula with the European continental territory, and located in the north of Catalonia;

(2) The Catalan Coastal mountain ranges or the Catalan Mediterranean System: an alternating elevations and planes parallel to the Mediterranean coast;

(3) The Catalan Central Depression: structural unit which forms the eastern sector of the Valley of the Ebro.


Figure 4. Physical map of study area (the red dotted line) in Catalonia

*3.2 Dataset Description*

The study area Catalonia is covered by a single S1 frame. In particular, two swaths and 7 bursts have been processed for monitoring measurement. The main characteristics of the processed dataset are presented in Table 1. S1 is a constellation composed of two twin satellites acquiring images at C-band (central frequency 5.4 GHz and wavelength 5.6 cm) which grants a 6-days revisiting cycle and 12-days for single satellite. The used SAR dataset consists of 111 S1 Wide Swath images spanning around two years period, with the first acquisition time in January 2017 and last one in January 2019. All the images from twin S1 satellites have been collected for measurement in this study, and the minimum temporal gap is 6 days, while the maximum is 12 days which is defined by the image available situation. Figure 5 shows all the acquisition times of the processed images and perpendicular baselines of interferograms.

As explained in the introduction, the aim of this paper is to generate the TS deformation maps for Catalonia because the deformation procedure is quite useful and important for the geohazard analysis. One interferometric network was designed with the minimal temporal baseline (6 days or 12 days due to the data downloading failure) to guarantee the coherences between these pairs shown in the Figure 5, which is the key point for interferograms generation with good quality.

The Shuttle Radar Topography Mission (SRTM) DEM provided by NASA has been utilized in coregistration and geocoding procedures to provide the interferometric products in this work (Blanco et al. 2012).

**Table 1** Main characteristics of the processed data

| **Name** | **Value** |
|---|---|
| **Satellite** | **Sentinel-1A** |
| Acquisition mode | Wide Swath |
| Minimum revisit period (days) | 6 |
| Wavelength ($\lambda$) (cm) | 5.55 |
| Polarization | VV |
| Full resolution (azimuth/range) (m) | 14/4 |
| Multi-look 1 × 5 resolution (azimuth/range) (m) | 14/20 |
| Multi-look 2 × 10 resolution (azimuth/range) (m) | 28/40 |
| Orbit | Descending |
| Incidence angle of the area of interest | $36.47^{\circ}$~$41.85^{\circ}$ |
| Period | January 2017~ January 2019 |

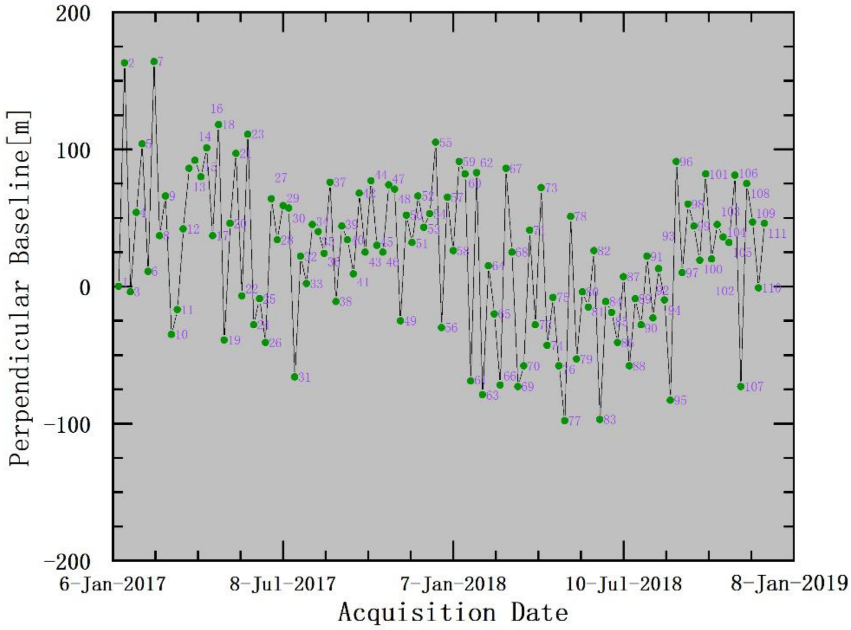


Figure 5. The time-baseline plot of the processed interferograms

### *3.1 Active Deformation results*

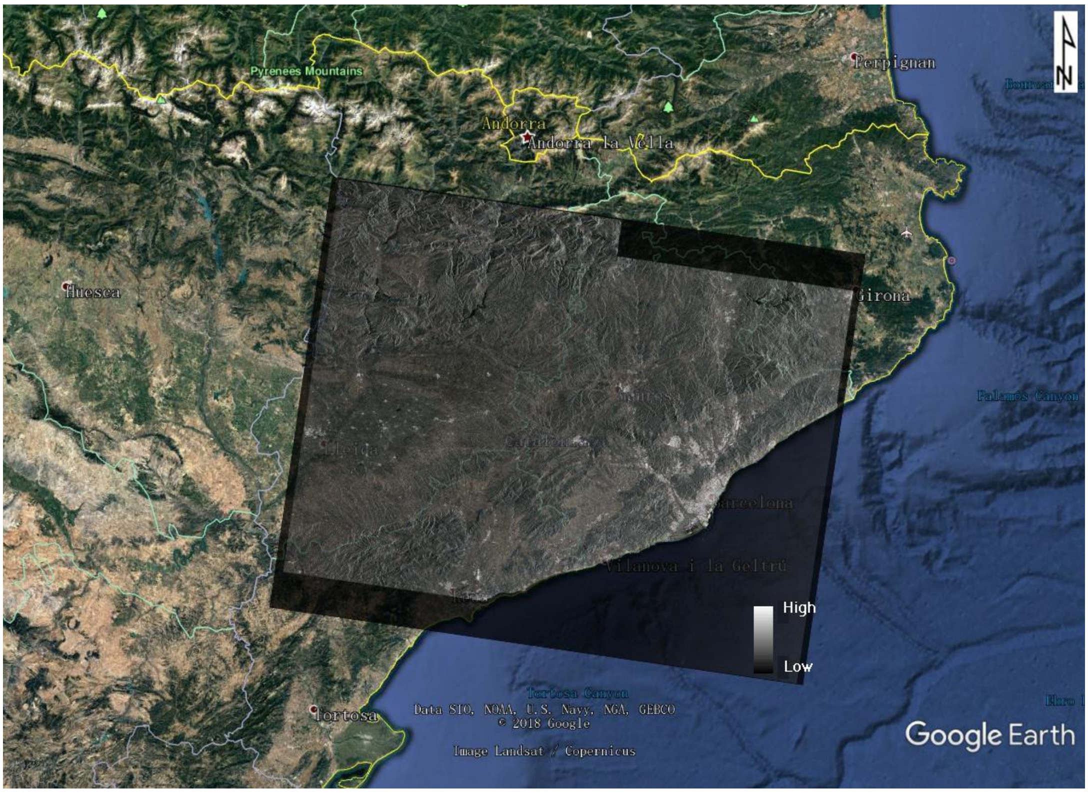


Figure 6. Footprint of the processed amplitude image and area of interest. The area is covered by 2 sub-swaths and 7 bursts

The monitoring results of this study concern a large part of Catalonia, see Figure 6. The covered area is approximately 19,000 km$^2$. 111 images have been processed by proposed method, the most part of interferograms has been affected by serious decorrelation and noise with the mean coherence less than 0.25(the threshold of PS candidates for PSI approach), see Figure 7(a), due to the vegetation coverage and topography. However, the active deformation results with excellent coverage could be generated using the proposed methodology, even for the active areas with large scale displacement in short time, such as mining area.

To analysis these deformation results in deep, some examples of these generated results over Catalonia are illustrated in Figure 7(b). Compared with results from traditional PSI techniques (Devanthéry et al. 2019), more than 5 million coherent points could be extracted for deformation monitoring with greater coverage which are valuable for civil risk evaluation and management. The accumulated deformation maps from some areas are shown along with a sample of the retrieved temporal deformation of a selected point among them. Three main deformation generator mechanisms have been identified at the affected areas in Catalonia:

(1) Underground mining activities are detected using the proposed method in intense ADA (towns of Súria, Cardona and Sallent among others) with great temporal serious accumulated settlements in Figure 8 and 9.

(2) Heavy surface load in the Barcelona Port and Airport whose subsidence has already been more than 10cm form January 2017 to January 2019. However, the dam nearby estuary of the EI LIobregat River has raised up more than 12cm in Figure 10 and 11.

(3) Intense water extraction is well recognized in some urban areas, most part of Igualada city is very stable, but there is a few subsidence in the downtown of this city might cause by water extraction or urban construction in Figure 12 and 13.

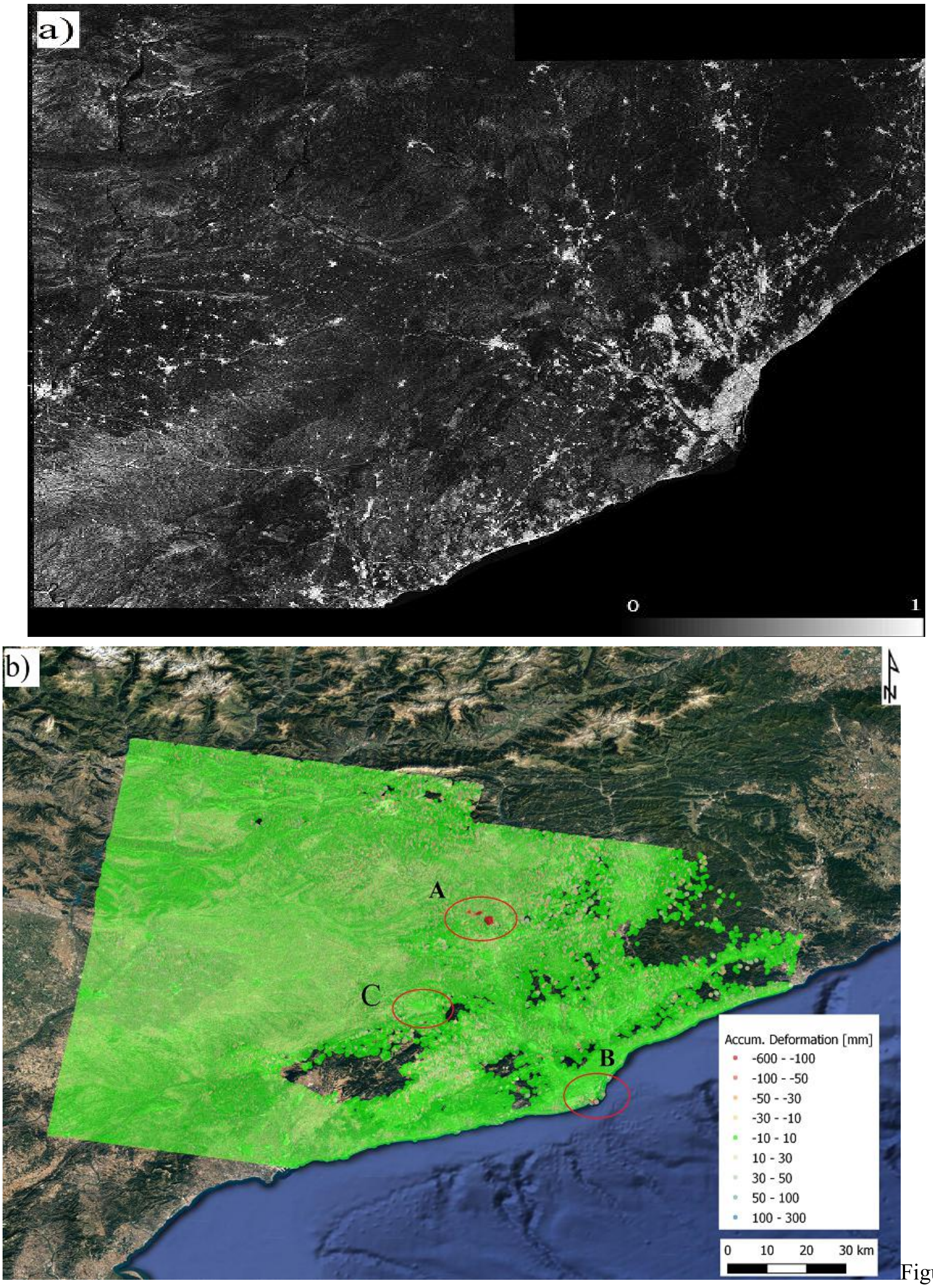


Figure 7. Mean coherence map (*a*) and accumulated deformation map (*b*) of study area. Three examples of deformation results will be presented (red circle)

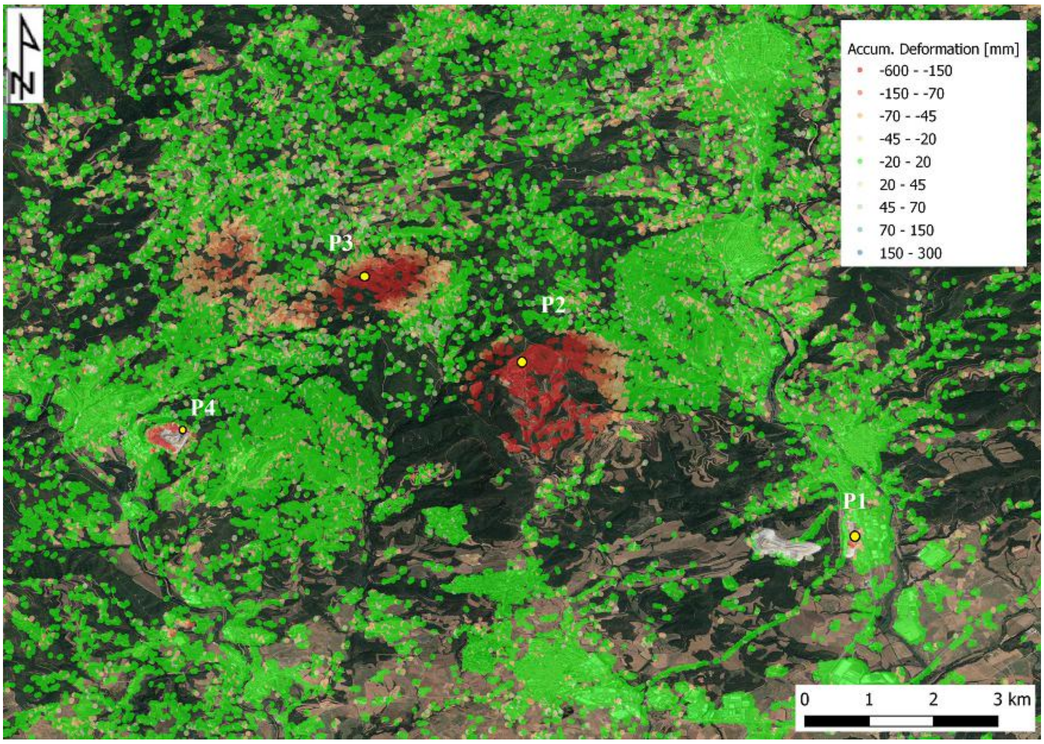


Figure 8. Active deformation map of area A revealing a surface subsidence (over -60 cm) caused by mining activities during observation period

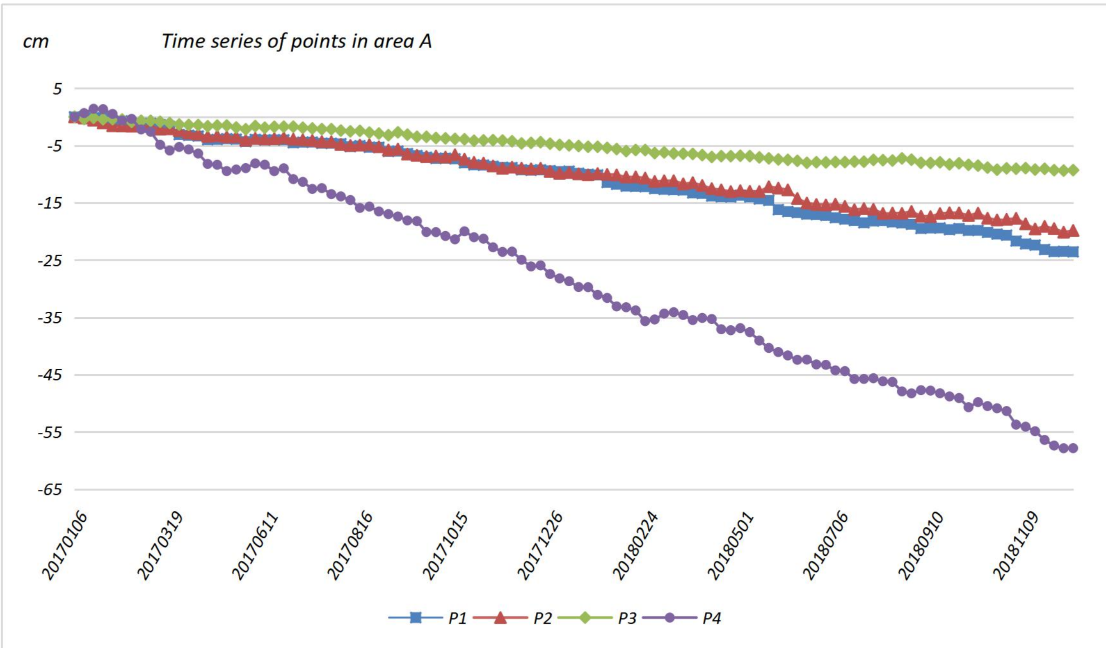


Figure 9. Four points of deformation results with time series located in the area A shown in Figure 8 (see yellow dots)


Figure 10. Active deformation map of area B (Barcelona Ports). P1 and P2 have surface subsidence (-2~-6 cm) due to surface loading during observation period, P3 has a lifting deformation (over 5 cm) caused by the sedimentation

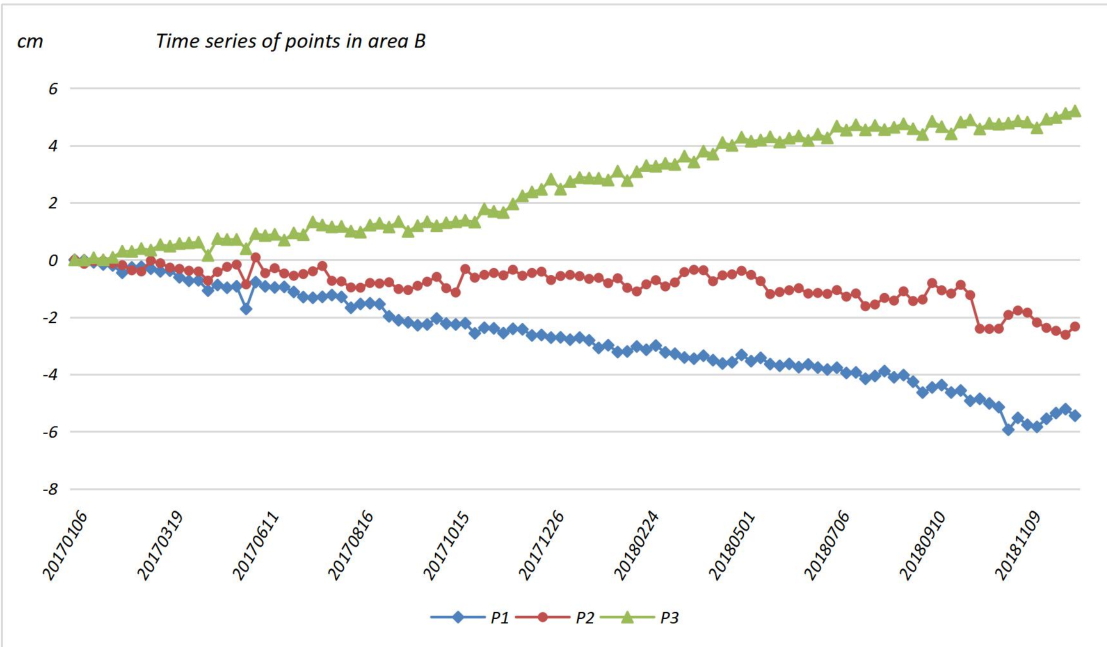


Figure 11. Three points of deformation results with time series located in the area B shown in Figure 10 (yellow dots)

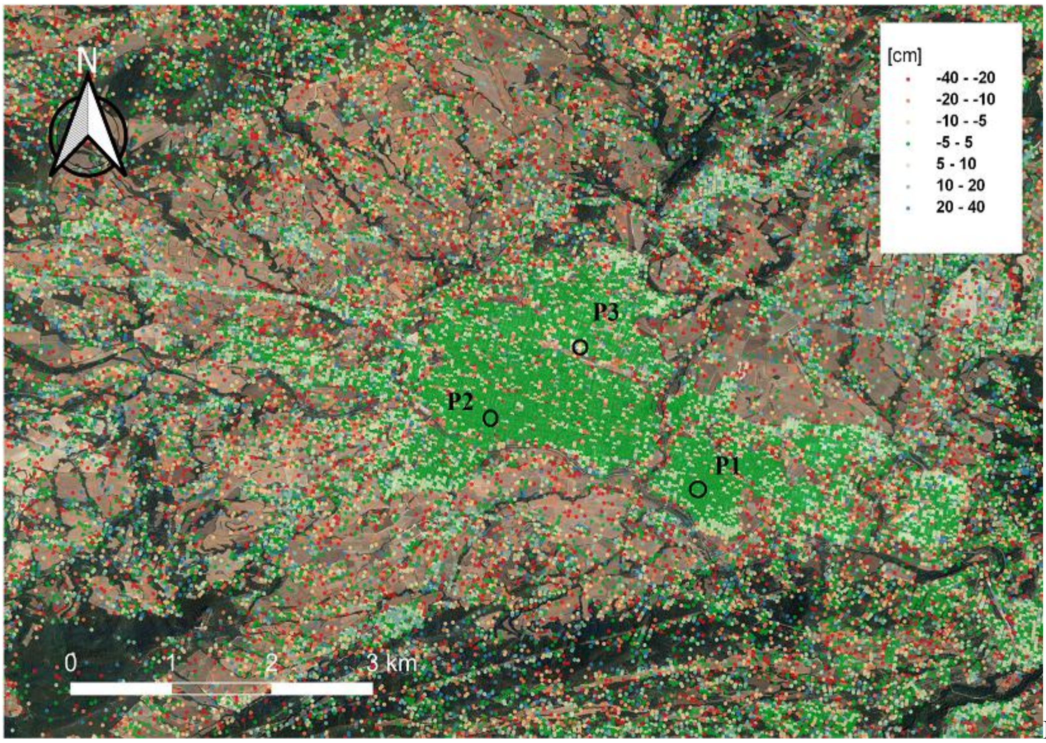


Figure 12. Active deformation map of area C (Igualada). P1 and P2 are all very stable during observation period, but P3 has a settlement (-13 cm) caused by the water extraction

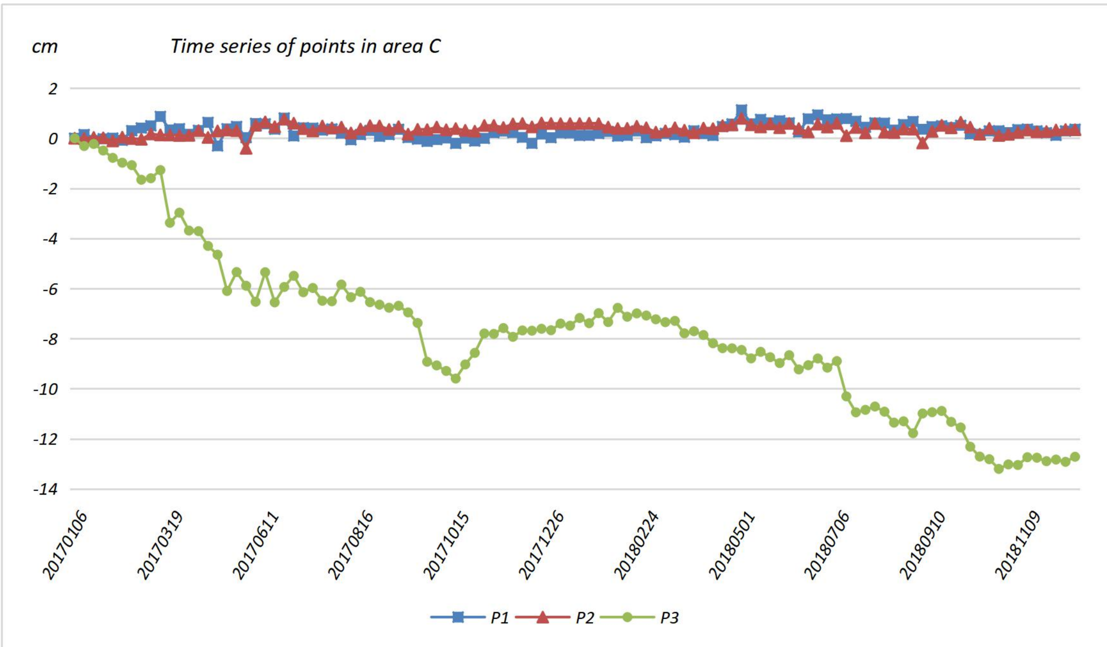


Figure 13. Three points of deformation results with time series located in the area C shown in Figure 12 (black circle)

## 4 Discussion

The methodology proposed in this work (Section 2) has been employed for the semi-automatic identification and pre-screening of deformational processes, and it was applied in the three case studies and the results are presented in the third section using S1 datasets and ancillary data (Section 3.2). The discussion is described in this section.

In this section, some key aspects, as well as the strengths and limitations of the presented methodology are commented. The presented methodology is aimed at generating active deformation maps with TS over wide areas, using the S1 images. The main challenge is to generate rapidly and semi-automatically a product to be easily exploited in the geohazard management by the Civil Protections and the Geological Surveys (P. Olea et al.2020).

The main advantage of the proposed method is the possibility of semi-automatically generating active deformation maps with TS to reveal the subsidence procedure for wide areas and break the maximum deformation detection ability of InSAR approach based on S1 datasets (Devanthéry et al. 2019). The output of the methodology is the TS deformation map which localizes only the most important detected active areas, unlike the conventional output of velocity map, which can contain all information of the interferometric phases without filtering and fitting process. The management and administration of the civil safety and the infrastructures can receive the support from this information of particular interests.

Furthermore, compared with other types of satellites, the better performances of the proposed methodology could be obtained using S1 satellite data with short revisit time of the S1, varying 6-12 days and allowing a wide area monitoring.

The methodology suffers the same inherent limitation of InSAR approach and SAR satellite data (Qiu et al. 2019; Yue et al. 2016). Apart from the theoretical drawback like acquisition geometry and displacement limitation, there are two other aspects that spatially influence the possibility of detecting movements: the frequency splitting process and the lack of noisy phase elimination.

## 5 Conclusions

In this paper a regional operational project in Catalonia (Spain) has been described with the objective to monitor surface deformation employing an Innovative Methodology and evaluate its geohazard safety for civil protection over wide areas (Tang et al. 2015; Bouali et al. 2016; Barhoux et al. 2014). DInSAR has proven to be an excellent tool for identifying affected areas at wide spatial scale. The aim of this project is to extract the deformation areas form the SAR satellite datasets in simple and fast way, specifically by the Civil Protection administrations in order to discover and avoid the risk of geohazard in time. The outputs of the methodology are the Deformation Areas Map (DAM) and the TS deformation, not only when evaluating the results but also to improve the PS-DInSAR processing strategy with an excellent coverage and point's density.

All the main steps of the methodology have been explained in this article, starting from the PSC selection, the high and low frequency split and integration of high and low parts to generate the DAM and the TS analysis of interesting PS points. The application and the results of the methodology over mining and ports areas in the Catalonia (Spain) have been presented and discussed. This innovative methodology improves the coverage and TS estimation of PS points greatly, yields a much better characterization of the deformation phenomena. The systematic integration of the results exhibits the regional scale monitoring potentialities of the proposed methodology, and the detailed TS analysis allows now and, in the future, a better understanding and quantification of the triggering mechanisms for geohazard evaluation purposes. Moreover, it is worthy to investigate and explore the real physical meaning of the threshold of HF and LF splitting adopted in our study. Considering the proper strategy suitable for other sensors and more experiments need to be verified in our future research.

## Acknowledgments

This work has been funded by the Belt and Road Special Foundation of the State Key Laboratory of Hydrology-Water Resources and Hydraulic Engineering [grant number 2018491411].

## Author Contributions

Zhiwei Qiu wrote the paper and was involved in the data processing and analysis; Michele Crosetto and Oriol Monserrat (CTTC) contributed in the SAR data processing and analysis of the results; Vrinda Krishnakumar provides the inputs analysis of Catalonia study test; Li Zhou modified the logical frame of this manuscript.

## Disclosure statement

No potential conflict of interest was reported by the authors.


## Funding

This work was supported by Scientific research project of Surveying and mapping geographic information in Jiangsu Province [JSCHKY201904].


**References**


Barboux, C.; Delaloye, R.; Lambiel, C. Inventorying slope movements in an Alpine environment using DInSAR. Earth Surf. Process. Landf. 2014, 39, 2087–2099.

Barra A, Solari L, Béjar-Pizarro M, et al. A methodology to detect and update active deformation areas based on sentinel-1 SAR images. Remote Sensing, 2017, 9(10): 1002.

Blanco, Pablo et al. "Operational PS-DInSAR deformation monitoring project at a regional scale in Catalonia (Spain)." 2012 IEEE International Geoscience and Remote Sensing Symposium, pp. 1178-1181, 2012.

Bouali, E.H.; Oommen, T.; Escobar-Wolf, R. Interferometric stacking toward geohazard identification and geotechnical asset monitoring. J. Infrastruct. Syst. 2016, 22, 05016001.

Crosetto, M., Monserrat, O., Muniganti, P., Sawicka, M., Rossi, G., Calcagni, L., & Crippa, B. A 2+ 1D phase unwrapping for advanced DInSAR data processing. In Proceedings of Fringe. 2007, pp.26-30.

Crosetto, M.; Monserrat, O.; Cuevas-González, M.; Devanthéry, N.; Crippa, B. Persistent scatterer interferometry: A review. ISPRS J. Photogramm. Remote Sens. 2016, 115, 78–89.

Crosetto, M.; Monserrat, O.; Iglesias, R.; Crippa, B. Persistent Scatterer Interferometry: Potential, limits and initial C- and X-band comparison. Photogramm. Eng. Remote Sens. 2010, 76, 1061–1069.

Daniel R, Marcello D M, Jean-Philippe M, et al. 2013. Time-variable 3D ground displacements from High-Resolution Synthetic Aperture Radar (SAR). Application to La Valette landslide (South French Alps). Remote Sensing of Environment, Elsevier. 139, pp.198-204.

Devanthéry, N., Crosetto, M., Monserrat, O., Cuevas-González, M., & Crippa, B. An approach to Persistent Scatterer Interferometry. Remote Sensing, 2014, 6, 6662–6679. doi:10.3390/rs6076662

Devanthéry N, Crosetto M, Monserrat O, et al. Data analysis tools for persistent scatterer interferometry based on Sentinel-1 data[J]. European Journal of Remote Sensing, 2019, 52(sup1): 15-25.

Ferretti A., Prati C. and Rocca F., “Permanent scatterers in SAR interferometry”, IEEE Transactions on Geoscience and Remote Sensing, Vol. 39(1) pp. 8–20, 2001.

Gabriel, A.K., Goldstein, R.M., Zebker, H.A. Mapping small elevation changes over large areas: Differential radar interferometry. J. Geophys. Res. 1989, 94, 9183–9191.

"Geological map of Catalonia". Institut Cartogràfic i Geològic de Catalunya. 2016. Retrieved 11 October 2017.

P. Olea, O. Monserrat, C. Sierralta, et al. "Mapping and monitoring ground instabilities with Sentinel-l data: the experience of Sernageomin," 2020 IEEE Latin American GRSS & ISPRS Remote Sensing Conference (LAGIRS), Santiago, Chile, 2020, pp. 421-427.

Qiu Z, Jiang T, Zhou L, et al. Study of subsidence monitoring in Nanjing City with small-baseline InSAR approach. Geomatics, Natural Hazards and Risk, 2019, 10(1): 1412-1424.

Qiu Z, Jiao M, Jiang T, et al. Dam Structure Deformation Monitoring by GB-InSAR Approach[J]. IEEE Access, 2020, (99):1-1.

Tang, P.; Chen, F.; Guo, H.; Tian, B.; Wang, X.; Ishwaran, N. Large-area landslides monitoring using advanced multi-temporal InSAR technique over the giant panda habitat, Sichuan, China. Remote Sens. 2015, 7, 8925–8949.

Yue J, Qiu Z, Wang X, et al. Atmospheric phase correction using permanent scatterers in ground-based radar interferometry. Journal of Applied Remote Sensing, 2016, 10(4): 046013.